Topics in Catalysis
https://doi.org/10.1007/s11244-022-01567-9

ORIGINAL PAPER

Electrocatalytic Analysis of Diclofenac in the Presence of Dopamine at Surface Amplified Voltammetric Sensor Based on Poly Glycine Modified Carbon Nano Tube Paste Electrode

B. M. Amrutha[1,2] · J. G. Manjunatha[1] · A. S. Bhatt[2] · N. Hareesha[1] · Abdullah A. Al-Kahtani[3] · Ammar Mohamed Tighezza[3] · Narges Ataollahi[4]

Accepted: 31 December 2021

Abstract
Diclofenac (DCF) is a non-steroidal anti-inflammatory drug used for the treatment of different diseases such as rheumatoid arthritis, spondylitis, arthritis and sport injuries. Increased use of DCF has initiated a significant worry regarding their presence in the environment. This study reports a sensitive and selective electrochemical sensing platform based on poly glycine modified carbon nanotube paste electrode (PGMCNTPE) for the simultaneous determination of DCF and dopamine (DA) by differential pulse voltammetry (DPV). The characterisation techniques like cyclic voltammetry (CV) and electrochemical impedance spectroscopy (EIS) accomplished in 1 mM K_4 [Fe $(CN)_6$], displays that the electroactive surface area of PGMCNTPE is augmented and the charge-transfer resistance is diminished in comparison to the bare carbon nanotube paste electrode (BCNTPE). Various parameters responsible for the peak improvement such as accumulation time, accumulation potential, pH and number of polymerisation cycles were optimised. Scan rate studies done by CV technique reveals that the process is irreversible and adsorption controlled in 0.2 M solution of phosphate buffer (PBS). The deposition of the poly glycine film on the BCNTPE surface enhanced the sensors electronic transfer rate, which reveals a heterogeneous rate constant (k_0) of 3.13×10^{-3} s^{-1}. PGMCNTPE shows two linear ranges with an increase in DCF concentration from 4 to 100 µM and a detection limit calculated by considering second linear range was found to be 0.21 µM. The selectivity of PGMCNTPE towards DCF was investigated in the existence of various interfering molecules and inorganic metal ions with fivefold higher concentration. The pertinence of the proposed sensor was analysed by quantification of DCF in pharmaceutical samples. The prepared sensor exhibits a virtuous performance in detection of DCF due to excellent repeatability, reproducibility and stability.

Keywords Poly glycine · Carbon nanotube paste · Voltammetry · Electronic impedance spectroscopy · Diclofenac

1 Introduction

DCF is a non-steroidal anti-inflammatory drug of wide use around the world with strong anti-pyretic, analgesic and anti-inflammatory properties. Humans suffering from inflammatory conditions like rheumatoid arthritis and osteoarthritis use DCF as a clinical medicine for their treatment [1]. Inflammatory diseases create a complex and heterogeneous group of diseases, which is a significant source of disability. DCF is a non-selective cyclo-oxygenase inhibitor belonging to a non-steroidal anti-inflammatory drug, with an extensive capacity to induce inflammation [2]. As an analgesic, it has a fast onset and an extended duration of action. DCF is commercially retailed in the name of Voltaren. Studies were conducted for a long time on the use of DCF by oral

✉ J. G. Manjunatha
manju1853@gmail.com

1 Department of Chemistry, FMKMC College, Constituent College of Mangalore University, Madikeri, Karnataka, India

2 Department of Chemistry, N.M.A.M. Institute of Technology, Visvesvaraya Technological University, Nitte, Udupi District, Belgavi, Karnataka 574110, India

3 Chemistry Department, College of Science, King Saud University, P. O. Box 2455, Riyadh 11451, Saudi Arabia

4 Department of Civil, Environmental and Mechanical Engineering, University of Trento, Via Mesiano, 77, 38123 Trento, Italy

Published online: 20 January 2022

consumption and topical administration. Analysis showed that topical administration was more effective to treat and caused minimal damage to the gastric, renal, liver and cardiac complications [3]. Once consumed, they are subjected to human metabolism. Overdose of DCF can lead to toxic side-effects. Health issues caused by the consumption of acidic pharmaceuticals by animals at low levels is not understood, but the decline in vulture population in Asia is reported due to DCF. It is also known as a compound that affects organ histology and gene expression in fish [4–9].

Considering the expansive pharmaceutical application of DCF, numerous methods have been established and practised over the last few years for quantitative and qualitative determination of DCF. Certain prominent methods include liquid chromatography–tandem mass spectrometry [10], spectrofluorimetry [11], gas chromatography-mass spectrometry [12], High performance liquid chromatography [13], Capillary electrophoresis [14], Spectrophotometry [15], Electroanalytical methods [16–18]. Electroanalytical methods prove to be more advantageous and a versatile analytical method due to their potential benefits like specificity, high sensitivity, easy sample preparation procedure which does not generally require the separation and extraction of interferents, relatively inexpensive instrumentation and usage of miniatured sensors.

Carbon nanotube (CNT) discovered in the year 1991, have been the target of many investigations due to their unique properties. CNT which are built from sp^2 carbon units present a seamless structure with hexagonal honeycomb lattices, being some nano-meters in diameter and several microns in length [19]. CNT which is known as buck tubes is composed of a concentric arrangement of numerous cylinders which has become as one of the strong studied nanostructured material [20–25]. CNT constitutes graphitic carbon comprising exceptional mechanical, electronic, and chemical properties. These properties make CNT very attractive for the task of electrochemical sensing. Recently, some studies showed that CNT can impart strong electrocatalytic activity and minimize surface fouling of the electrode [26].

The redox path at the BCNTPE occur at over potential due to slow electron transfer rate. To enhance the electrocatalytic behaviour of CNT, the electrode surface has to be modified by the conductive catalytic material. Surface modification reduces the over potential and increases the electron transfer rate at the electrode and the analyte interface [27]. Using polymers as modifiable material for electrode surface, has involved enormous attention in electroanalysis [22–24, 28–32]. The basic properties of polymers like stability, biocompatibility and homogeneity have attracted a lot of consideration in electro catalysis. Poly amino acids play a pivotal role in drug delivery, sensor fabrication and environmental analysis. Glycine (GLY) an important proteinogenic amino acid, is a building block for protein that has a single hydrogen atom as its side chain [33]. Research has proved that Poly (GLY) has favourable electro catalysis effects [34]. Electrochemical polymerization of GLY on the surface of BCNTPE is a preferable and affordable method because of its advantages like modest preparation process, consistency in electrochemical deposition, good selectivity, excellent sensitivity, superior stability and robust adhering ability to the surface of the electrode [35–38]. Hence, PGMCNTPE is used for the specific sensitive determination of DCF in the presence of DA.

2 Experimental

2.1 Instrumentation

Electrochemical analyser CHI-6038E model (CH Instruments, Inc. Austin, USA) was used at an ambient temperature to study the electrochemical activities of the analyte under investigation. This analyser is integrated with an electrochemical cell consisting of three electrodes in which PGMCNTPE and BCNTPE of 3 mm diameter acts as a working electrode, KCl saturated calomel electrode and platinum wire from Equiptronics (Mumbai, Maharashtra, India), acts as a reference electrode and auxiliary electrode respectively.

2.2 Chemicals and Reagents

All the commercially available chemicals used are of highest quality and are used without further purification. DCF was purchased from Molychem, Mumbai, India. DA, Potassium hex cyanoferrate (II) trihydrate and Potassium chloride (KCl) were procured from Sigma Aldrich, India. Silicone oil (used as a binder), GLY, Sodium salts of monobasic phosphate and dibasic phosphate were obtained from Nice chemicals, Ernakulam, Kerala, India. Multi walled carbon nanotubes (MWCNTs) used for the electrode fabrication with a dimension of 30–50 nm and length 10–30 µM was purchased from Sisco Research Laboratory Ltd. Maharashtra, India. DCF, DA (25×10^{-4} M) and GLY (25×10^{-3} M) stock solutions were prepared by dissolution of appropriate quantity of respective chemicals in distilled water. 0.2 M PBS solution of required pH, was prepared by inter mixing the desired quantity of NaH_2PO_4 (0.2 M) and Na_2HPO_4 (0.2 M).

2.3 Preparation of BCNTPE and PGMCNTPE

Carbon nanotube paste (CNTP) was prepared by mixing CNT powder and silicone oil in the proportion of 60% and 40%, mass percentages was mixed thoroughly in the agate

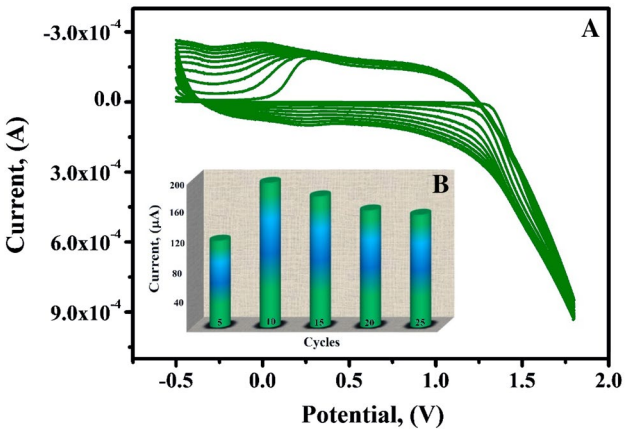

Fig. 1 **A** Cyclic voltammogram of electrochemical polymerisation of 1×10^{-3} M GLY in 0.2 M PBS of pH 5.7 within the potential window − 0.6 V to 1.8 V at a scan rate 0.1 V/s. **B** Plot of the oxidative peak current of 1×10^{-3} M GLY versus the number of polymerization cycles

mortar with the help of a pestle to get a consistent mixture. For voltammetry assays the resultant mixture was filled firmly into the teflon tube of 3 mm diameter. To get a smooth surface and to avoid incorporation of air bubbles the electrode surface prior to modification was rubbed on a smooth tissue paper. Hence, BCNTPE with homogeneous surface was obtained. A copper wire implanted into the teflon tube enables a connection between the analyte and the electrochemical analyser. Voltammetric modification of CNTPE was achieved by running ten sequential cycles of cyclic voltammetry in PBS of pH 5.7 containing 1×10^{-3} M GLY. The poly (GLY) film was deposited on the surface of BCNTPE in the potential gap of − 0.6 to + 1.8 V. After each voltammetric assay, the working electrode surface was replenished by removing the superficial layer of carbon nano tube paste.

3 Results and Discussions

3.1 Electrochemical Polymerisation of GLY

The PGMCNTPE was fabricated by running uninterrupted ten CV cycles (scan rate of 0.1 V/s) in 0.2 M PBS of pH 5.7 containing 1×10^{-3} M GLY. Figure 1A shows effective polymerisation within the potential window − 0.6 to + 1.8 V. The redox current was found to increase progressively in each of CV cycles, which confirms the development of electroactive polymer film of poly (GLY) over the electrode surface [39]. The nitrogen atom in amino group of GLY forms a strong nitrogen—carbon linkage with the carbon atom at the electrode surface. During electro polymerization, one hydrogen radical is eliminated along with the formation of GLY free radical and in turn the GLY free radical formed gets attached to the BCNTPE surface. The attached molecule thus interacts with another GLY molecule with the removal of water molecule and the length of the polymer chain increases. The probable electrochemical polymerisation is represented in Fig. 2. The polymer film deposited on the BCNTPE was methodically rinsed with double distilled water to eliminate traces of GLY monomer.

The extent of thickness of the polymer film on the electrode surface has a substantial impact on the current sensitivity of the target electroactive species. Poly GLY film of different thickness were obtained by varying the number of scan cycles from 5 to 25. Figure 1B clearly indicates that the peak currents of DCF in 0.2 M PBS of pH 7 ($v = 0.1$ V/s) increased up to 10 scan cycles and thereafter showed a steady decline. As the thickness of the polymer film on the electrode surface increases the electron transfer rate decreases due to the deficient disclosure of reactive sites on the electrode. Therefore 10 repetitive scan cycles were fixed as an optimum condition for the fabrication of PGMCNTPE.

3.2 Surface Topography Studies of Working Electrodes by FE-SEM

The surface topography of the CNT based working sensor was examined using FE-SEM. FE-SEM images of randomly aligned CNTs before and after electro polymerisation of poly (GLY) are shown in Fig. 3A and B, respectively. Figure 3A displays a densely packed surface which exposes a characteristic tube-like structure of CNTs. After electro polymerization of GLY on the BCNTPE surface, a porous structure was visualised (Fig. 3B). The formation of the flake-like structure and variations in the topography of the BCNTPE supported the formation of poly GLY on the bare surface which establishes the development of active sites [40].

3.3 Electronic Impedance Studies

EIS spectra of 1 mM $K_4[Fe(CN)_6]$ in 0.1 M KCl was recorded for the proposed sensor before and after modification with

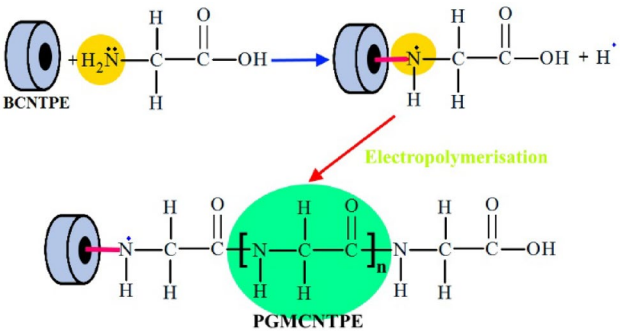

Fig. 2 Probable electro polymerisation mechanism of GLY

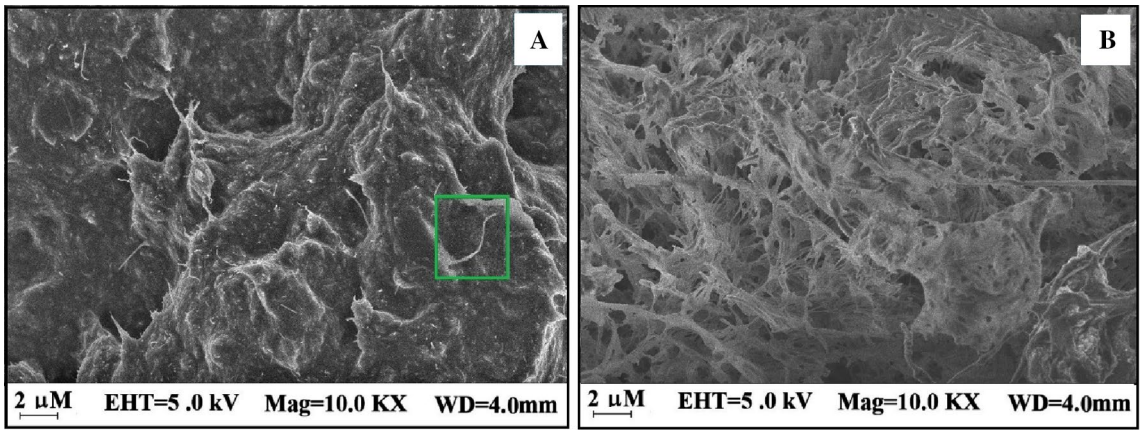

Fig. 3 **A** FE-SEM image of BCNTPE. **B** FE-SEM image of PGMCNTPE

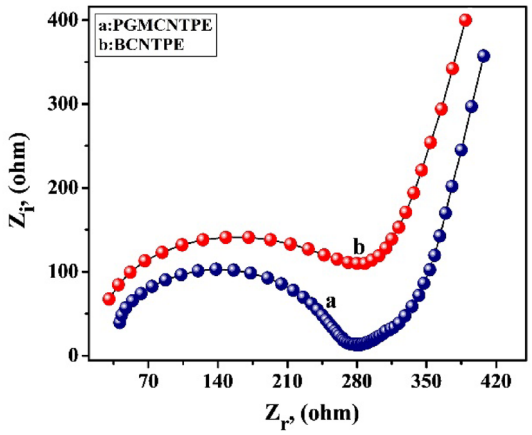

Fig. 4 Nyquist diagrams of EIS of PGMCNTPE (curve a) and BCNTPE (curve b)

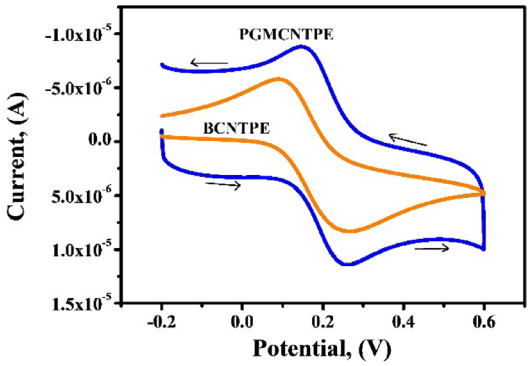

Fig. 5 Cyclic voltammograms of 1 mM $K_4[Fe(CN)_6]$ at BCNTPE and PGMCNTPE in 0.1 M KCl at a scan rate of 0.1 V/s

an intent of obtaining information about the electron transfer kinetics (R_{ct}) between the electrode—solution interface. Figure 4 displays the Nyquist plot concerning to EIS which has two parts where the linear part present at lower frequencies represents the diffusion-controlled process and the semicircular portion present at higher frequencies corresponds to electron transfer limited process [41]. R_{ct} value is dependent on the diameter of the semicircle and from the Nyquist plot (Fig. 4) it is observed that the semi-circular portion of BCNTPE is larger than that of PGMCNTPE. R_{ct} value of BCNTPE is 100.6 kΩ and the R_{ct} value for PGMCNTPE is 5.9 kΩ which signifies that the polymer film formed on the bare electrode surface is presumed to enhance the conductance of the modified sensor.

3.4 Evaluation of Electrode Surface Area

The rate of a reaction and peak current is proportional to the electrochemically active surface area of the fabricated electrode. The electrochemically active surface areas of BCNTPE and PGMCNTPE were evaluated by considering the peak current density obtained for the reversible redox couple like $[Fe(CN)_6]^{3-}/[Fe(CN)_6]^{4-}$ by CV. The obtained peak current, was used in the Randles–Sevcik equation (Eq. 1) to calculate the electrochemically active surface area of the working electrodes.

$$I_{pa} = 2.69 \times 10^5\, n^{3/2}\, A\, C_o\, D^{1/2}\, \nu^{1/2} \quad (1)$$

n: electron transfer number (n = 1) during the redox reaction, A(cm^2): surface area of the fabricated electrode, D(cm^2/s): diffusion coefficient, C_o (mol/cm^2): concentration of the redox probe and ν (V/sec): potential sweep rate. On substituting the significant values, the electroactive surface area of PGMCNTPE was found to be 0.048 cm^2

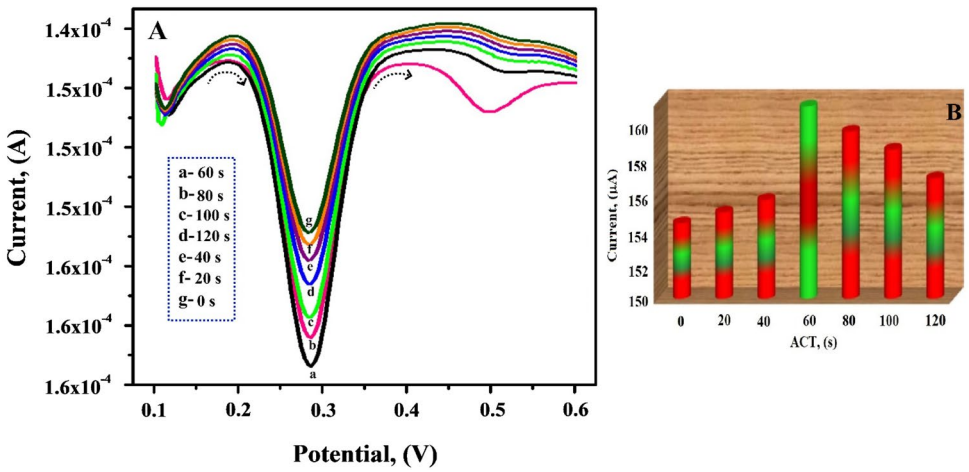

Fig. 6 **A** Differential pulse voltammograms obtained for 1×10^{-4} M DCF at various ACT ranging from 0 to 120 s in 0.2 M PBS of pH 7. **B** Plot of anodic peak current of 1×10^{-4} M DCF at PGMC-NTPE as a function of ACT

while that of BCNTPE was 0.025 cm^2. Figure 5 displays that the oxidation and reduction peak currents of modified electrode (scan rate of 0.1 V/s) was more sensitive and well-defined with an anodic and cathodic peak potential difference (ΔEp) of 0.110 V. However, for BCNTPE the current sensitivity decreased but the ΔEp value increased to 0.165 V. This voltammetric display validates that the activated surface of the modified electrode shows the enhanced catalytic role due to the increase in electroactive surface area and the GLY polymer film enable the conducting bridges for the electron-transfer. The ratio of I_{pa}/I_{pc} remained unity and this specifies that the Fe (II) to Fe (III) transformation is a reversible process [42, 43].

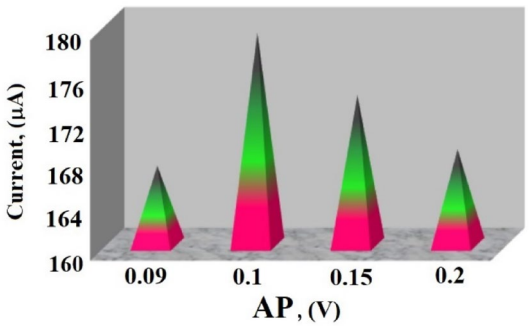

Fig. 7 Plot of anodic peak current of 1×10^{-4} M DCF at PGMC-NTPE as a function of accumulation potential in 0.2 M PBS of pH 7 at a scan rate of 0.1 V/s

3.5 Optimisation of Accumulation Time and Accumulation Potential

Accumulation time (ACT) has the tendency to provide efficient electrochemical response with enhanced sensitivity. Hence, the effect of ACT from 0 to 120 s on the oxidation peak current of DCF was analysed in 0.2 M PBS of physiological pH. The DPV recorded at various ACT is depicted in Fig. 6A. The peak current of DCF increased with the increase in ACT from 0 to 60 s then showed a steady decline with further increase in ACT up to 120 s. The maximum current sensitivity was obtained at 60 s, signifying a full surface coverage of PGMCNTPE and later it leads to saturated adsorption [44, 45]. Therefore, the plot between peak current and ACT (Fig. 6B) reveals that 60 s is the optimum ACT.

Figure 7 depicts the plot between accumulation potential (AP) and peak current. From the plot it was observed that the current sensitivity shows an increase in peak current with the shift in potential from 0.09 to 0.1 V and with the later shift in potential from 0.15 to 0.2 V the peak current shows a decline. Hence an AP of 0.1 V was chosen as an optimum condition for subsequent determinations.

3.6 Effect of pH

Protonation mechanism of organic species will have substantial effect on the redox process and hence the optimisation of pH was assessed by DPV. The effect of the supporting electrolyte on the electro-oxidation of DCF was investigated in the solutions of different pH ranging from 5.5 to 8. The highest peak sensitivity was found in pH 7.0 (Fig. 8A), and low electrochemical response of DCF in higher pH was observed due to the lack of sufficient protons. Linear relationship was observed in the plot of E_{pa} vs. pH (Fig. 8B) where with the increase in pH the oxidative peak potentials steadily declined towards the less positive side and the linear shift in peak potential was probably due to the deprotonation process involved in the oxidation of the analyte. The linear regression equation can be expressed as, E_{pa} (V) = 0.605 − 0.045 pH with R^2 = 0.9972. The slope value gives an idea of the involvement of electrons and protons. The probable electrochemical mechanism is represented in Fig. 9. According to

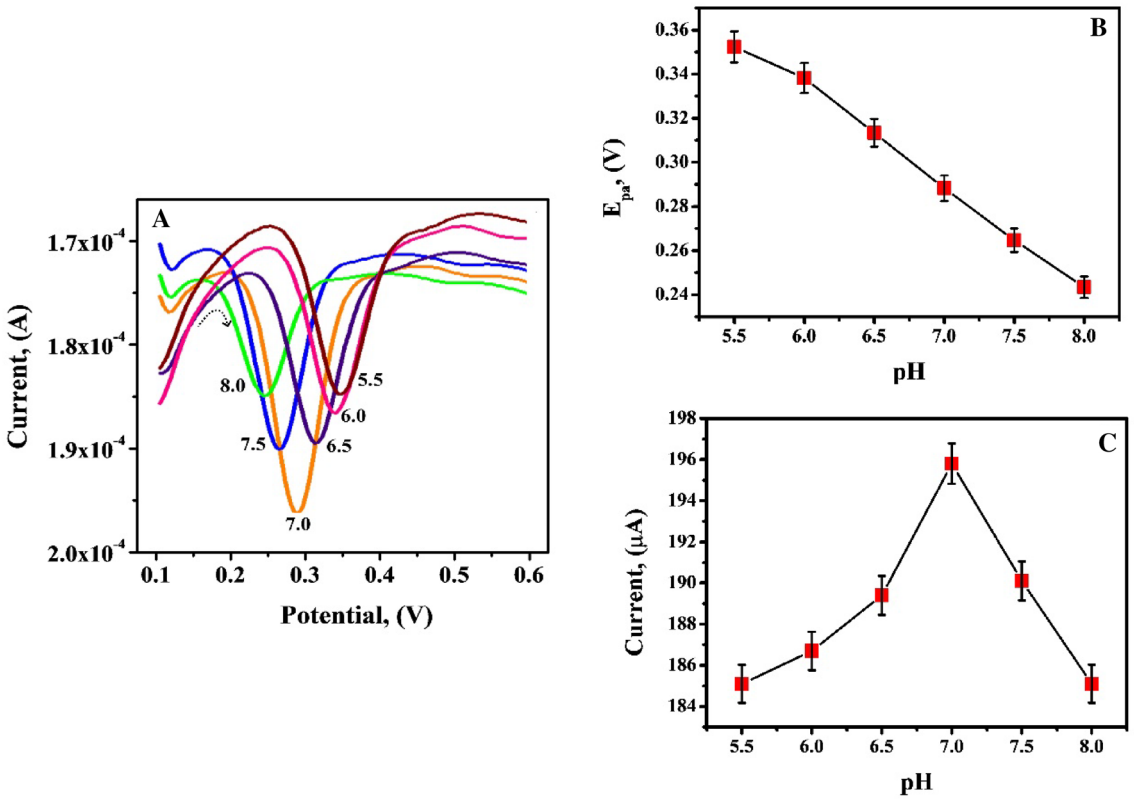

Fig. 8 **A** DPV response of 1×10^{-4} M DCF at PGMCNTPE in 0.2 M PBS of pH in the range 5.5–8.0 at a scan rate of 0.1 V/s. **B** Plot of anodic peak potential (E_{pa}) vs pH. **C** Plot of oxidation peak current (I_{pa}) versus pH of solution

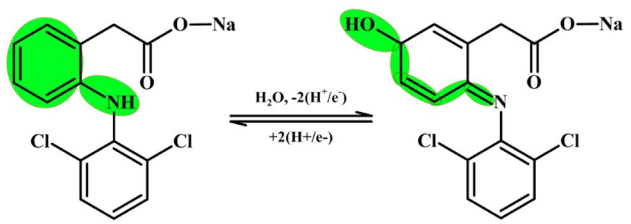

Fig. 9 Proposed redox mechanism of DCF

the plot of Ipa vs pH (Fig. 8C) the peak current increases from pH 5.5 to 7 and after that the peak current shows a decline. The most favourable electro-oxidation of DCF was obtained at physiological pH and hence pH 7 was considered optimum for further investigations [46, 47].

3.7 CV, DPV and LSV Behaviour of DCF at PGMCNTPE

The electrochemical behaviour of 1×10^{-4} M DCF was analysed by CV in 0.2 M PBS of pH 7. Figure 10A shows the CV at PGMCNTPE and BCNTPE, where PGMCNTPE shows two oxidation peaks, but the peak at a potential of 0.382 V is sharp with an enhanced current sensitivity of 106.0 µA and a reduction peak is obtained at a potential of 0.250 V with a current sensitivity of − 103.0 µA. The potential difference (ΔEp) between these two peaks is greater than 0.059 V and hence it implies that the electrochemical reaction of DCF is quasi-reversible. But in contrast, BCNTPE under alike condition exhibits a diminished current sensitivity due to the slower rate of electron transfer [48].

DPV shows higher current sensitivity and sharp resolution compared to CV. Figure 10B shows the DPV of DCF (1×10^{-4} M) at the modified sensor and the bare electrode at a scan rate of 0.1 V/s. PGMCNTPE in contrary to BCNTPE, shows an enhanced current sensitivity at a potential of 0.288 V with a peak current of 195.8 µA [49].

Linear sweep voltammetry (LSV) investigation of 1×10^{-4} M DCF was performed under optimised condition (Fig. 10C). As per the observation from LSV, the modified sensor displays enhanced current sensitivity of 89.05 µA at a potential of 0.369 V. The increase in electroanalytical signal at PGMCNTPE by all the three methods was due to the electro-oxidation of DCF with enhanced electrochemical kinetics. The polymeric layer of poly (GLY) with large number of active sites acts as an proficient promoter in the transfer of electrons.

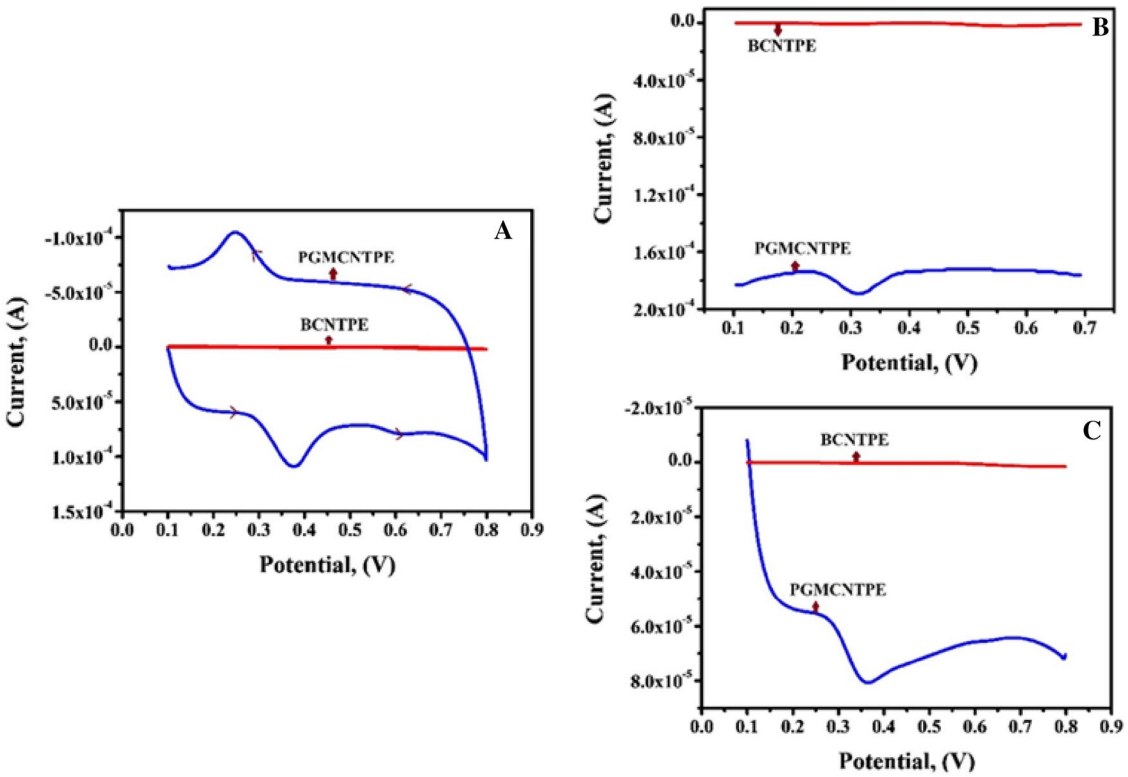

Fig. 10 **A** CV response of 1×10^{-4} M DCF at BCNTPE and PGMCNTPE at a scan rate of 0.1 V/s in 0.2 M PBS of pH 7. **B** DPV response of 1×10^{-4} M DCF at BCNTPE and at PGMCNTPE under optimum condition. **C** LSV response of 1×10^{-4} M DCF at the surface of BCNTPE and PGMCNTPE under optimum condition

3.8 Influence of Scan Rate

The study of scan rate influence on various parameters like the speed at which reaction proceeds, the type of process taking place at the electrode surface, reaction pathways and number of electrons transferred were analysed by CV method [50]. Figure 11A displays the CV for the variation of scan rate from 0.025 to 0.20 V/s for the oxidation of 1×10^{-4} M DCF in 0.2 M PBS of pH 7.0 at PGMCNTPE. The PGMCNTPE showed increase in the peak current signals with increasing scan rate along with the shift in anodic peak potential to the more positive side. Electron transfer rate is considered to be slow if the extent of the peak potential separation increases and this slower rate increases with the upsurge of scan rate. The linearity observed in the plot of I_{pa} versus scan rate (Fig. 11B) signifies that the process is adsorption-controlled. The corresponding equation can be stated as I_{pa} (μA) = 7.668 + 911.5 v (V/s); $R^2 = 0.9932$. Linearity was observed between log I_{pa} and log υ (Fig. 11C), and the corresponding equation can be stated as log I_{pa} = 2.997 log υ + 1.008; $R^2 = 0.9932$. The slope value of 1.008 is close to the anticipated value for adsorption-controlled electrode process. Linearity between the plot of E_{pa} and log υ (Fig. 11D) displays relatively linear relationship with regression equation $E_{pa} = 0.467 + 0.080 \log v$; $R^2 = 0.9924$.

The heterogeneous rate constant (k_0) value was found to be 3.13×10^{-3} s^{-1} which was calculated by using the experimental peak potential difference (ΔEp) in Eq. 2 [51];

$$\Delta Ep = 201.39\log\left(\upsilon/k_0\right)301.78 \tag{2}$$

Number of electrons, 'n' participating in the electrochemical reaction of DCF was calculated by using the Laviron expression (Eq. 3) was found to be 1.70 and was considered to be two [52].

$$E_{pa} = K + \frac{RT}{(1-a)nF}\ln v \tag{3}$$

The value of charge transfer coefficient α was calculated by using Bard and Faulkner equation (Eq. 4) which was found to be 0.54 [53].

$$\Delta E_p = \frac{47.7}{an} \tag{4}$$

Surface concentration (Γ) was evaluated by using Eq. 5 [54]:

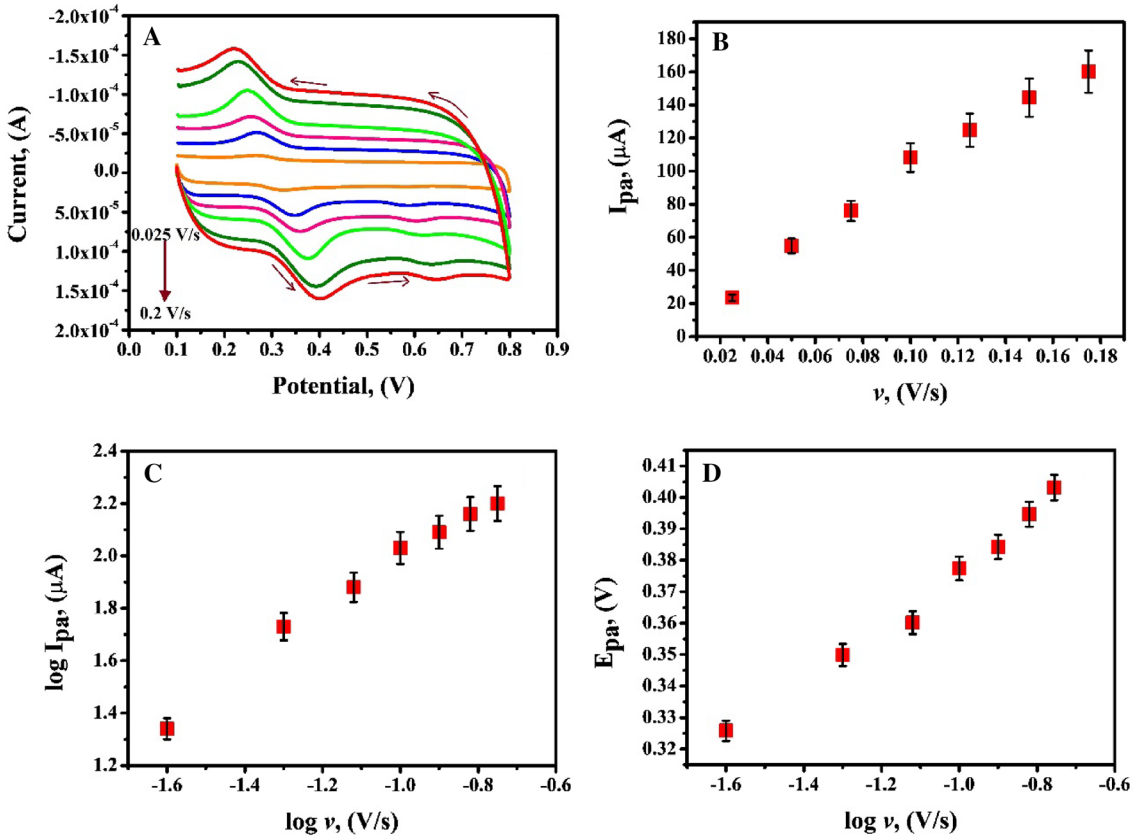

Fig. 11 **A** CV response of 1×10^{-4} M DCF at PGMCNTPE in 0.2 M PBS of pH 7 at various scan rates from (0.025 to 0.200 V/s). **B** Plot of I_{pa} vs v. **C** Plot of log I_{pa} vs log v. **D** Plot of E_{pa} vs log v

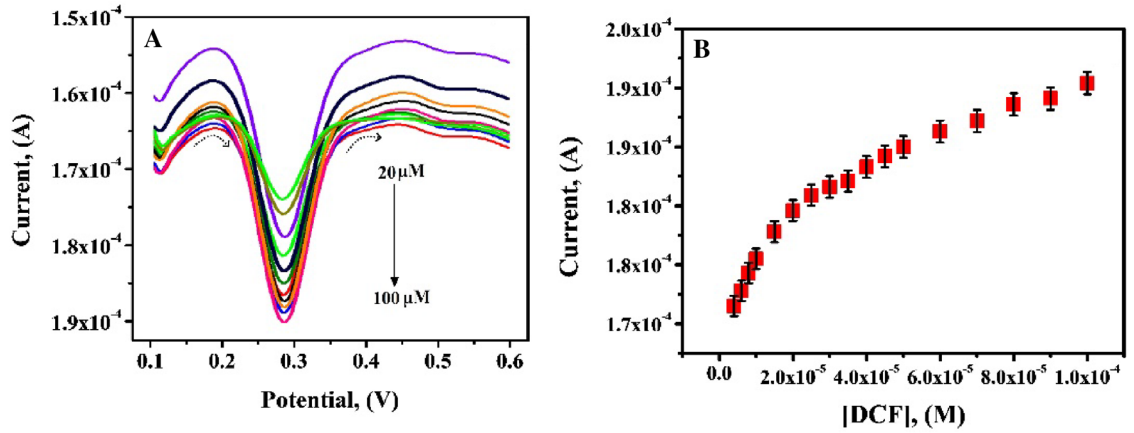

Fig. 12 **A** DPV curve for the variation of concentration of 1×10^{-4} M DCF in 0.2 M PBS of pH 7 at PGMCNTPE. **B** Calibration plot between anodic peak current values of DCF and the altered concentrations of DCF at PGMCNTPE in 0.2 M PBS of pH 7 at a scan rate of 0.1 V/s

$$Q = \Gamma nFA \quad (5)$$

The evaluated value of Γ was found to be 2.80 nmol/cm^2.

3.9 Calibration Curve and Detection Limit

Under the optimized experimental conditions relationship between the oxidation peak current and DCF concentration was analysed by DPV since sharper and better-defined

Table 1 Comparative study of the LOD values of PGMCNTPE with previously reported sensor for voltammetric analysis of DCF

Electrode	Linear range (M)	Detection limit (M)	Method	Reference
CNTPE[a]	2–100 µ	0.8 µ	NPV[b]	[56]
IL/CNTPE[c]	0.5–300 µ	0.2 µ	DPV	[57]
MWCNT-IL|CCE[d]	0.05–50 µ	0.018 µ	DPV	[58]
BDDE[e]	5–50 µ	0.14 µ	FIA[f]	[59]
Plasticized/ISE[g]	10–1000 µ	4.0 µ	Potentiometry	[60]
CuZEGE[h]	0.2–30 µ	0.05 µ	CV	[61]
DyNW/CPE[i]	0.01–1 µ	2.0 n	FFT SWV[j]	[62]
PGMCNTPE	20–100 µ	0.21 µ	DPV	Present work

[a]Carbon nanotube paste electrode

[b]Normal pulse polarography

[c]Ionic liquid-modified carbon nanotubes paste electrode

[d]Multiwalled carbon nanotube and ionic liquid-modified carbon ceramic electrode

[e]Boron-Doped Diamond Electrode

[f]Flow-Injection Amperometric

[g]Plasticised ion selective electrode

[h]Cu-doped zeolite-modified expanded graphite-epoxy composite electrode

[i]Dysprosium nano wire carbon paste electrode

[j]Fast Fourier Transform Square-Wave Voltammetry

peaks were observed at lower concentrations of DCF than those obtained by cyclic voltammetry. Figure 12A demonstrates that the peak current increased with the increasing concentration of DCF but the peak potential remained unaltered. The calibration plot (Fig. 12B) shows two linear ranges within the concentration range of 4 to 100 µM. Underneath the optimised preconditions the linearity equation for the first linear range from 4 to 15 µM, is expressed as I_{pa} (µA) = $1.777 \times 10^{-4} + 0.132$ [DCF] (M); ($R^2 = 0.9903$) and for the second linear range from 20 to 100 µM the equation is expressed as I_{pa} (µA) = $1.694 \times 10^{-4} + 0.574$ [DCF] (M); ($R^2 = 0.9986$). The LOD and LOQ values calculated by using second linear range and was found to be 0.21 µM and 0.71 µM respectively. (LOD = 3S/N, LOQ = 10 S/N where S and N represents the standard deviation of 5 voltammograms and slope of calibration plot) [55]. The experimentally obtained results for detection of DCF at PGMCNTPE are compared in Table 1 with other electrodes reported in the referral publications. The compared value of linear range and LOD of the present electrode is in par with certain electrodes but depicts lower LOD than certain electrodes.

3.10 Simultaneous Determination of DCF Along with DA

The selectivity of PGMCNTPE for the analysis of DCF was investigated by considering any sort of interference encountered from endogenic substances like DA. DA is a vital neurotransmitter that is present in the central nervous system of mammals. It plays a pivotal role in biological and pharmacological processes. Variation in DA levels is associated with diseases like Parkinson's which is caused by the neural inflammation leading to degradation of DA level. DCF is a commonly used nonsteroidal anti-inflammatory drug that swiftly cross blood brain barriers and stimulates nuclear factor peroxisome proliferator which is a neuroprotector [63, 64]. The effect of DCF was considered for its antidepressant effect in diverse in vivo and in-vitro models of rats. DCF was found to restore DA levels by preventing neuronal loss and cellular damage in Parkinson's model through its anti-inflammatory effects [65]. DA belongs to catecholamine group and it is readily oxidised like DCF because of which it is well characterized by its electrochemical activity [66]. Hence, under optimal condition the equipped sensor was effectively used to determine DCF and DA (1×10^{-4} M) simultaneously. From Fig. 13A it was observed that PGMCNTPE exhibited enhanced current sensitivity with well resolved peaks at a potential of 0.1444 V for DA and at 0.2974 V for DCF.

Figure 13B displays the DPV obtained by changing the concentration of DCF and DF simultaneously. The peak current of DCF and DA increased with the increase in the concentrations from 10 µM to 60 µM, respectively. Plot of I_{pa} versus the concentration of DCF (Fig. 13C) exhibits a respectable linear relation and the calculated LOD value in the presence of DA at PGMCNTPE was 0.46 µM, which is almost nearer to the LOD value obtained in the absence

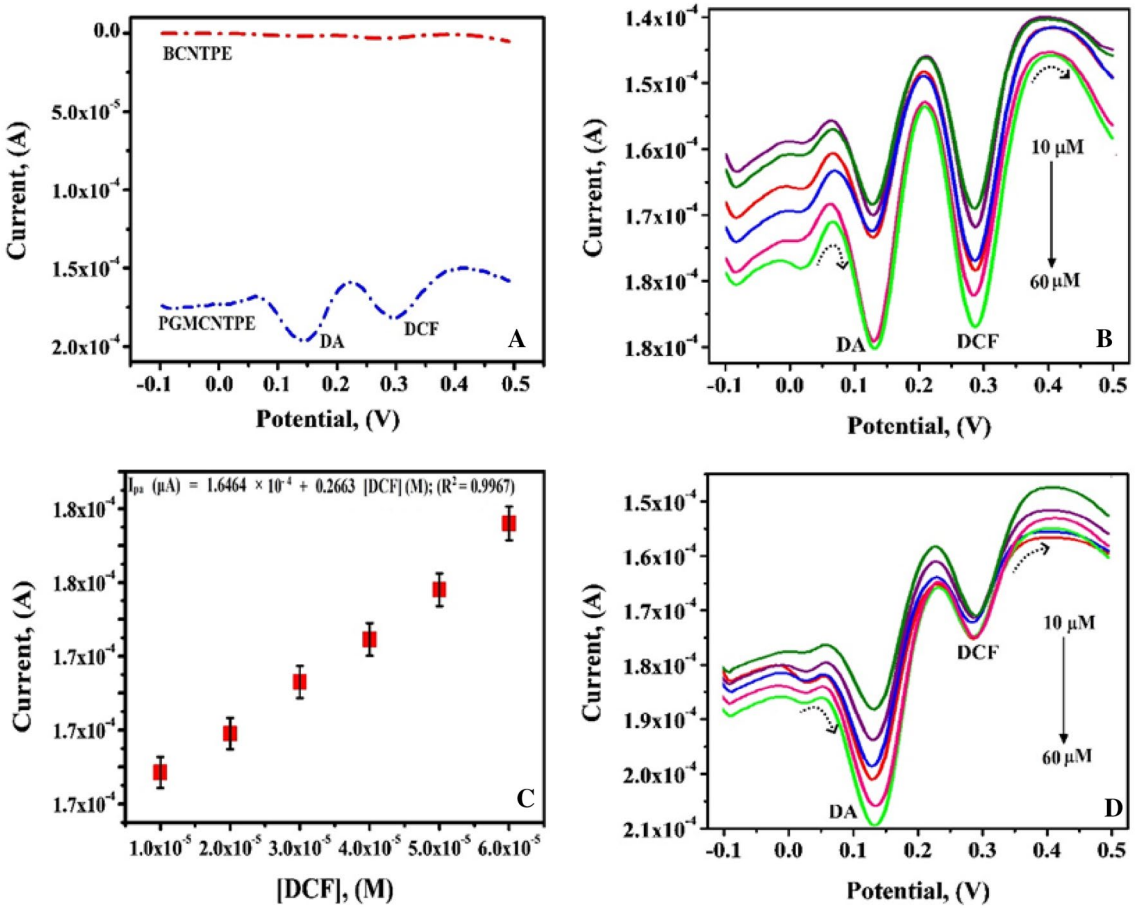

Fig. 13 **A** DPV response for simultaneous determination of DA and DCF (1×10^{-4} M) at PGMCNTPE and BCNTPE in 0.2 M PBS of pH 7 at a scan rate of 0.1 V/s. **B** DPV response for simultaneous analysis with varying concentration from 10 to 60 µM of DA and DCF in 0.2 M PBS of pH 7 at a scan rate of 0.1 V/s. **C** Plot of I_{pa} vs concentration variation of DCF under optimum condition. **D** DPV response for simultaneous analysis by DCF (concentration kept constant) and DA (concentration varied) in 0.2 M PBS of pH 7 at a scan rate of 0.1 V/s

of DA. Figure 13D shows the DPV response which was obtained by increasing the DA concentration from 10 µM to 60 µM while keeping the DCF concentration constant. The peak current response of DA increased linearly while the current response of 10 µM DCF remained unaltered. Hence, PGMCNTPE can be used for simultaneous determination of DCF and DA, since DCF responses at the detection base is not relative to the presence of DA.

3.11 Interference Studies

Pharmaceutical samples contain certain inactive substance formed along with the active component of the prescribed medication, which will have a significant impact on the selectivity of the modified electrodes [67, 68]. DPV analysis of DCF (1×10^{-4} M) at PGMCNTPE was done under optimized condition in the existence of highly concentrated solutions of certain foreign substance like uric acid, glucose, urea, starch and ascorbic acid. The selectivity of the modified sensor was also studied by adding some cations like Fe^{3+}, K^+, Mg^{2+}, Na^+, Ca^{2+} which are biologically present in human body. The results showed that the presence of potential interferents does not have impact on the oxidation potential of DCF and hence PGMCNTPE can be effectively used for the specific determination of DCF.

3.12 Stability, Repeatability and Reproducibility

Stability of the PGMCNTPE was evaluated by documenting 30 CV cycles under optimised experimental condition. The experimental outcome obtained exhibited that 86% of the initial current signal was retained. The repeatability of the proposed sensor for DCF sample of different concentrations was assessed by intraday study through CV measurements. The relative standard deviation (RSD) was found to

Table 2 Recovery data of DCF tablet sample

Sample	Added (10^{-6} M)	Found (10^{-6} M)	Recovery (%)
DCF tablet sample	10	9.87	98.73
	20	19.97	99.88
	30	30.03	100.10

be 3.23% (n = 3) which signifies that equipped PGMCNTPE has high repeatability with good shelf-life and precision. The reproducibility of the proposed sensor was also investigated via intraday study, by independently fabricating the modified electrode for five times and the CV data of DCF sample under identical condition was recorded each time. The calculated RSD value of 3.45% signifies that PGMCNTPE maintains good reproducibility which is an essential aspect for analytical applications.

3.13 Analytical Application of PGMCNTPE

DCF tablet (from local drug store) was crushed into fine powder using a pestle and mortar. Suitable amount of the tablet powder was dissolved in deionised water and then filtered to get a clear solution. Considering the dilution factor different concentration of clear filtrate solution was added to 0.2 M PBS of pH 7 and the DPVs were recorded at PGMCNTPE. From the experimental outcome recovery was calculated and a good percentage of recovery was obtained in the tablet with a mean recovery of 99.57% (Table 2) which justifies the noteworthy application of PGMCNTPE in determination of DCF in pharmaceutical sample.

4 Conclusion

PGMCNTPE displays a significant role in simultaneous determination of DCF and DA by DPV method. The surface characterisation of the proposed sensor was accomplished by FE-SEM, EIS and CV. The modified sensor exhibits definite characteristics like strong adsorptive property, enlarged active surface area of 0.048 cm^2, soaring conductivity with upgraded sensitivity. When compared to BCNTPE, PGMCNTPE shows strong electro catalytic activity in the electro-oxidation of DCF with a high current sensitivity. Scan rate studies revealed that the process was adsorption controlled and reversible in 0.2 M PBS of pH 7 with a heterogeneous rate constant (k_0) of 3.13×10^{-3} s^{-1}. LOD value achieved was found to be 0.21 µM. The developed sensor's analytical applicability was proved by employing it to analyse potential interferents and determine DCF in a pharmaceutical sample. The general analytical performance of PGMCNTPE was determined to be beneficial because to its accuracy, simplicity of instrumentation, and quick analysis procedure.

Funding (1) N. Hareesha, thankfully acknowledge the financial support to the Department of Science and Technology (DST), for the INSPIRE Fellowship (Registration number: IF180479). (2) Abdullah A. Al-Kahtani and Ammar Mohamed TIGHEZZA grateful to the Researchers Supporting Project Number (RSP-2021/266), King Saud University, Riyadh, Saudi Arabia.

Declarations

Conflict of interest The authors don't have any conflict of interest.

References

1. Yilmaz B, Kaban S, Akcay BK, Ciltas U (2015) Differential pulse voltammetric determination of diclofenac in pharmaceutical preparations and human serum. Braz J Pharm Sci 51:285–294. https://doi.org/10.1590/S1984-82502015000200005
2. Da-Cunha CEP, Rodrigues ESB, Alecrim MF, Thomaz DV, Macedo IYL, Jeronimo LFG, Neto RDO, Moreno EKG, Ballaminut N, Gi EDS (2019) Voltammetric evaluation of diclofenac tablets samples through carbon black-based electrodes. Pharmaceuticals 12:1–11. https://doi.org/10.3390/ph12020083
3. Honakeri NC, Malode SJ, Kulkarni RM, Shetti NP (2020) Electrochemical behaviour of diclofenac sodium at coreshell nanostructure modified electrode and its analysis in human urine and pharmaceutical samples. Sensors 1:100002. https://doi.org/10.1016/j.sintl.2020.100002
4. Madikizela LM, Chimuka L (2017) Simultaneous determination of naproxen, ibuprofen and diclofenac in wastewater using solid-phase extraction with high performance liquid chromatography. Ajol 43:1–11. https://doi.org/10.4314/wsa.v43i2
5. Shashanka R, ParhamT ACK, Orhan U, Emre A, Gururaj KJ (2021) Photocatalytic degradation of rhodamine B (RhB) dye in waste water and enzymatic inhibition study using cauliflower shaped ZnO nanoparticles synthesized by a novel one-pot green synthesis method. Arab J Chem 14:103180. https://doi.org/10.1016/j.arabjc.2021.103180
6. Gururaj KJ, Roberto FM (2018) Regioselectivity in hexagonal boron nitride co-doped graphene. New J Chem 42:18913–18918. https://doi.org/10.1039/C8NJ03679A
7. Adimule V, Nandi SS, Jagadeesha Gowda AH (2021) Enhanced power conversion efficiency of the P3BT (poly-3-butyl thiophene) doped nanocomposites of Gd-TiO3 as working electrode. Springer, Cham. https://doi.org/10.1007/978-3-030-69925-3_6
8. Adimule V, Bowmik D, Adarsha HJ (2020) A facile synthesis of Cr doped WO3 nanocomposites and its effect in enhanced current-voltage and impedance characteristics of thin films. Lett Mater 10:481–485. https://doi.org/10.22226/2410-3535-2020-4-481-485
9. Adimule V, Yallur BC, Sharma K (2021) Studies on crystal structure, morphology, optical and photoluminescence properties of flake-like Sb doped Y2O3 nanostructures. J Opt. https://doi.org/10.1007/s12596-021-00746-3
10. Sparidans RW, Lagas JS, Schinkel AH, Schellens JHM, Schellens JH, Beijnen JH (2008) Liquid chromatography-tandem mass spectrometric assay for diclofenac and three primary metabolites in mouse plasma. J Chromatogr A 872:77–82. https://doi.org/10.1016/j.jchromb.2008.07.012

11. Pandey G (2013) Spectrophotometric methods for estimation of diclofenac sodium in tablets. Int J Biomed Adv Res 4:77–82. https://doi.org/10.7439/ijbar
12. Yilmaz B (2010) GC–MS determination of diclofenac in human plasma. Chromatographia 71:549–551. https://doi.org/10.1365/s10337-010-1479-z
13. Chmielewsk A, Konieczn L, Plenis A, Bieniecki M, Lamparczyk H (2006) Determination of diclofenac in plasma by high performance liquid chromatography with electrochemical detection. Biomed Chromatogr 20:119–124. https://doi.org/10.1002/bmc.537
14. Jin W, Zhang J (2000) Determination of diclofenac sodium by capillary zone electrophoresis with electrochemical detection. J Chromatogr A 868:101–107. https://doi.org/10.1016/S0021-9673(99)01149-8
15. Mitic S, Miletic G, Pavlovic A, Tosic S, Pecev E (2007) Determination of diclofenac sodium in commercial pharmaceutical formulations and human control serum using a kinetic-spectrophotometric method. Chem Pharm Bull 55:1423–1426. https://doi.org/10.1248/cpb.55.1423
16. Kamenicka B, Bartaskova A, Svancara I, Weidlich T (2019) Applicability of voltammetric determination of diclofenac at carbon paste electrodes to the analysis of aqueous solutions purified by adsorption and/or ionic liquid-based ion exchange. Monatsh Chem 150:429–437. https://doi.org/10.1007/s00706-019-2354-8
17. Goyal RN, Chatterjee S, Agrawal B (2010) Electrochemical investigations of diclofenac at edge plane pyrolytic graphite electrode and its determination in human urine. Sens Actuators B: Chem 145:743–748. https://doi.org/10.1016/j.snb.2010.01.038
18. Hareesha N, Manjunatha JG, Amrutha BM, Pushpanjali PA, Charithra MM, Prinith SN (2021) Electrochemical analysis of indigo carmine in food and water samples using a poly (glutamic acid) layered multi-walled carbon nanotube paste electrode. J Electron Mater 50:1230–1238. https://doi.org/10.1007/s11664-020-08616-7
19. Rubianes MD, Rivas GA (2003) Carbon nanotubes paste electrode. Electrochem Commun 5:689–694. https://doi.org/10.1016/S1388-2481(03)00168-1
20. Shashanka R, Yasemin K, Recep T, Yusuf C, Ali S, Orhan U, Abdullah CK (2019) Antimicrobial investigation of CuO and ZnO nanoparticles prepared by a rapid combustion method. Phys Chem Res 7:799–812. https://doi.org/10.22036/PCR.2019.199338.1669
21. Gururaj KJ, Roberto FM (2017) Quantum chemical study of triton X-100 modified graphene surface. Electrochim Acta 248:225–231. https://doi.org/10.1016/j.electacta.2017.07.109
22. Adimule V, Nandi SS, Yallur BC, Bhowmik D, Jagadeesha AH (2021) Enhanced photoluminescence properties of Gd (x–1) Sr x O: CdO nanocores and their study of optical, structural, and morphological characteristics. Mater Today Chem 20:100438. https://doi.org/10.1016/j.mtchem.2021.100438
23. Adimule V, Yallur BC, Bhowmik D, Jagadeesha AH (2021) Morphology, structural and photoluminescence properties of shaping triple semiconductor YxCoO:ZrO2 nanostructures. J Mater Sci: Mater Electron 32:12164–12181. https://doi.org/10.1007/s10854-021-05845-2
24. Adimule V, Yallur BC, Kamat V, Krishna PM (2021) Characterization studies of novel series of cobalt (II), nickel (II) and copper (II) complexes: DNA binding and antibacterial activity. J Pharm Investig 51:347–359. https://doi.org/10.1007/s40005-021-00524-0
25. Amrutha BM, Manjunatha JG, Bhatt AS, Malini K (2021) Sodium dodecyl sulfate modified carbon nano tube paste electrode for sensitive cyclic voltammetry determination of Isatin. Adv Pharm Bull 11:111–119. https://doi.org/10.34172/apb.2021.012
26. Wang J, Musameh M (2004) Electrochemical detection of trace insulin at carbon-nanotube-modified electrodes. Anal Chim Acta 511:33–36. https://doi.org/10.1016/j.aca.2004.01.035
27. Amrutha BM, Manjunatha JG, Aarti SB (2020) Design of a sensitive and selective voltammetric sensor based on a cationic surfactant-modified carbon paste electrode for the determination of alloxan. ACS Omega 5:23481–23490. https://doi.org/10.1021/acsomega.0c03517
28. Pushpanjali PA, Manjunatha JG, Amrutha BM, Hareesha N (2020) Development of carbon nanotube-based polymer-modified electrochemical sensor for the voltammetric study of curcumin. Mater Res Innov. https://doi.org/10.1080/14328917.2020.1842589
29. Shashanka R, Debasis C, Dibyendu C (2016) Fabrication of nano-yttria dispersed duplex and ferritic stainless steels by planetary milling followed by spark plasma sintering and non-lubricated sliding wear behaviour study. J Mater Sci Eng B 6:111–125. https://doi.org/10.17265/2161-6221/2016.5-6.001
30. Shashanka R, Abdullah CK, Ceylan Y, Orhan U (2020) A fast and robust approach for the green synthesis of spherical magnetite (Fe 3 O 4) nanoparticles by *Tilia tomentosa* (Ihlamur) leaves and its antibacterial studies. Pharm Sci 26:175–183. https://doi.org/10.34172/PS.2020.5
31. Isha S, Pankaj K, Shruti S, Gururaj KJ (2021) A short review on electrochemical sensing of commercial dyes in real samples using carbon paste electrodes. Electrochem 2:274–294. https://doi.org/10.3390/electrochem2020020
32. Adimule V, Revaigh MG, Adarsha HJ (2020) Synthesis and fabrication of Y-doped ZnO nanoparticles and their application as a gas sensor for the detection of ammonia. J Mater Eng Perform 29:4586–4596. https://doi.org/10.1007/s11665-020-04979-4
33. Yu AM, Zhang HL, Chen HY (1997) Fabrication of a PolyGLY chemically modified electrode and its electrocatalytic oxidation to ascorbic acid. Electroanalysis 9:788–790. https://doi.org/10.1002/elan.1140091011
34. Shaoying-He P-H, Zhang X, Zhang X, Li K, Jia L, Dong F (2018) Poly(GLY)/graphene oxide modified glassy carbon electrode: preparation, characterization and simultaneous electrochemical determination of dopamine, uric acid, guanine and adenine. Anal Chim Acta 1031:75–82. https://doi.org/10.1016/j.aca.2018.06.020
35. Shashanka R (2018) Effect of sintering temperature on the pitting corrosion of ball milled duplex stainless steel by using linear sweep voltammetry. Anal Bioanal Electrochem 10:349–361
36. Adimule V, Nandi SS, Yallur BC, Bhowmik D, Jagadeesha AH (2021) Optical, structural and photoluminescence properties of Gd x SrO: CdO nanostructures synthesized by Co precipitation method. J Fluoresc 31:487–499. https://doi.org/10.1007/s10895-021-02683-7
37. Adimule V, Revaiah R, Nandi S, Jagadeesha A (2020) Synthesis, characterization of Cr doped TeO2 nanostructures and its application as EGFET PH sensor. Electroanalysis 33:579–590. https://doi.org/10.1002/elan.202060329
38. Adimule V, Yallur BC, Bhowmik D, Gowda AHJ (2021) Dielectric properties of P3BT doped ZrY2O3/CoZrY2O3 nanostructures for low-cost optoelectronics applications. Trans Electr Electron Mater. https://doi.org/10.1007/s42341-021-00348-7
39. Palakollu VN, Thapliyal N, Chiwunze TE, Karpoormath R, Karunanidhi S, Cherukupalli S (2017) Electrochemically reduced graphene oxide/Poly-GLY composite modified electrode for sensitive determination of L-dopa. Mater Sci Eng C 77:394–404. https://doi.org/10.1016/j.msec.2017.03.173
40. Wayu MB, Di-Pasquale LT, Schwarzmann MA, Gillespie SD, Leopold MC (2016) Electropolymerization of beta-cyclodextrin onto multi-walled carbon nanotube composite films for enhanced selective detection of uric acid. J Electroanal Chem 783:192–200. https://doi.org/10.1016/j.jelechem.2016.11.021
41. Charithra MM, Manjunatha JG (2020) Electrochemical sensing of paracetamol using electropolymerised and sodium lauryl sulfate modified carbon nanotube paste electrode. Chem Sel 5:9323–9329. https://doi.org/10.1002/slct.202002626

42. Mbokou SF, Pontie M, Bouchara JP, Tchieno FMM, Njanja E, Mogni A, Pontalier PY, Tonle IK (2016) Electroanalytical performance of a carbon paste electrode modified by coffee husks for the quantification of acetaminophen in quality control of commercialized pharmaceutical tablets. Int J Electrochem. https://doi.org/10.1155/2016/1953278
43. Amrutha BM, Manjunatha JG, Bhatt AS, Pushpanjali PA (2020) Fabrication of a sensitive and selective electrochemical sensing platform based on poly-l-leucine modifed sensor for enhanced voltammetric determination of Ribofavin. J Food Meas Charact 14:3633–3643. https://doi.org/10.1007/s11694-020-00608-9
44. Madej M, Kochana J, Bas B (2019) Determination of viloxazine by differential pulse voltammetry with boron-doped diamond electrode. Monatsh Chem 150:1655–1665. https://doi.org/10.1007/s00706-019-2380-6
45. Elqudabya HM, Mohamed GG, Ali FA, Eid SM (2013) Validated voltammetric method for the determination of some antiprotozoa drugs based on the reduction at an activated glassy carbon electrode. Arab J Chem 6:327–333. https://doi.org/10.1016/j.arabjc.2011.05.019
46. Beitollahi H, Maleh HK, Khabazzadeh H (2008) Nanomolar and selective determination of epinephrine in the presence of norepinephrine using carbon paste electrode modified with carbon nanotubes and novel 2-(4-Oxo-3-phenyl-3,4-dihydro-quinazolinyl)-N′-phenyl-hydrazinecarbothioamide. Anal Chem 80:9848–9851. https://doi.org/10.1021/ac801854j
47. Manjunatha JG (2018) A novel poly (GLY) biosensor towards the detection of indigo carmine: a voltammetric study. J Food Drug Anal 26:292–299. https://doi.org/10.1016/j.jfda.2017.05.002
48. Beitollahi H, Maleh HK, Khabazzadeh H (2008) Nanomolar and selective determination of epinephrine in the presence of norepinephrine using carbon paste electrode modified with carbon nanotubes and novel 2-(4-Oxo-3-phenyl-3,4-dihydro-quinazolinyl)-N-phenyl-hydrazinecarbothioamide. Anal Chem 80:9848–9851. https://doi.org/10.1021/ac801854j
49. Almbrok EM, Yusof NA, Abdullah J, Zawawi RM (2020) Electrochemical behaviour and detection of diclofenac at a microporous Si3N4 membrane modified water–1,6-dichlorohexane interface system. Chemosensors 8:1–11. https://doi.org/10.3390/chemosensors8010011
50. Raril C, Manjunatha JG (2020) A simple approach for the electrochemical determination of vanillin at ionic surfactant modified graphene paste electrode. Microchem J 154:104575. https://doi.org/10.1016/j.microc.2019.104575
51. Avendano SC, Angeles GA, Ramirez-Silva MT, Pina GR, Romo MR, Pardave MP (2007) On the electrochemistry of dopamine in aqueous solution. Part I: the role of [SDS] on the voltammetric behaviour of dopamine on a carbon paste electrode. J Electroanal Chem 609:17–26. https://doi.org/10.1016/j.jelechem.2007.05.021
52. Hareesha N, Manjunatha JG (2020) Fast and enhanced electrochemical sensing of dopamine at cost-effective poly (DL-phenylalanine) based graphite electrode. J Electroanal Chem 878:114533. https://doi.org/10.1016/j.jelechem.2020.114533
53. Bard AJ, Faulkner LR (2021) Electrochemical methods: fundamentals and applications, 2nd edn. Wiley, New York
54. Razmi H, Harasi M (2008) Voltammetric behaviour and amperometric determination of ascorbic acid at cadmium pentacyanonitrosyl ferrate film modified glassy carbon electrode. Int J Electrochem Sci 3:82–95
55. Prinith NS, Manjunatha JG, Raril C (2019) Electrocatalytic analysis of dopamine, uric acid and ascorbic acid at poly (adenine) modified carbon nanotube paste electrode: a cyclic voltammetric study. Anal Bioanal Electrochem 11:742–756
56. Ambrosi A, Antiochia R, Campanella L, Dragone R, Lavagnini I (2005) Electrochemical determination of pharmaceuticals in spiked water samples. J Hazard Mater 122:219–225. https://doi.org/10.1016/j.jhazmat.2005.03.011
57. Ensafi AA, Izadi M, Maleh HK (2013) Sensitive voltammetric determination of diclofenac using room-temperature ionic liquid-modified carbon nanotubes paste electrode. Ionics 19:137–144. https://doi.org/10.1007/s11581-012-0705-0
58. Sarhangzadeh K, Khatami AA, Jabbari M, Bahari S (2013) Simultaneous determination of diclofenac and indomethacin using a sensitive electrochemical sensor based on multiwalled carbon nanotube and ionic liquid nanocomposite. J Appl Electrochem 43:1217–1224. https://doi.org/10.1007/s10800-013-0609-3
59. Gimenes DT, Freitas JM, Munoz RAA, Richter EM (2011) Flow-injection amperometric method for determination of diclofenac in pharmaceutical formulations using a boron-doped diamond electrode. Electroanalysis 23:2521–2525. https://doi.org/10.1002/elan.201100126
60. Kormosh ZA, Hunka IP, Baze YR (2009) An ion-selective sensor for assay of diclofenac in medicines. Pharm Chem J. 43:428–430. https://doi.org/10.1007/s11094-009-0311-2
61. Manea F, Ihos M, Remes A, Burtica G, Schoonman J (2010) Electrochemical determination of diclofenac sodium in aqueous solution on Cu-doped zeolite-expanded graphite-epoxy electrode. Electroanalysis 22:2058–2063. https://doi.org/10.1002/elan.201000074
62. Daneshgar P, Norouzi P, Ganjali MR, Dinarvand R, Movahedi AAM (2009) Determination of diclofenac on a dysprosium nanowire- modified carbon paste electrode accomplished in a flow injection system by advanced filtering. Sensors 9:7903–7918. https://doi.org/10.3390/s91007903
63. Naeem S, Najam R, Khan SS, Mirza T, Sikandar B (2019) Neuroprotective effect of diclofenac on chlorpromazine induced catalepsy in rats. Metab Brain Dis 34:1191–1199. https://doi.org/10.1007/s11011-019-00416-1
64. Makunts T, Cohen IV, Lee KC, Abagyan R (2018) Population scale retrospective analysis reveals distinctive antidepressant and anxiolytic effects of diclofenac, ketoprofen and naproxen in patients with pain. PLoS ONE 13:1–10. https://doi.org/10.1371/journal.pone.0195521
65. Oni J, Nyokong T (2001) Simultaneous voltammetric determination of dopamine and serotonin on carbon paste electrodes modified with iron (II) phthalocyanine complexes. Anal Chim Acta 434:9–21. https://doi.org/10.1016/S0003-2670(01)00822-4
66. Manjunatha JG, Jayaprakash GK (2019) Electrooxidation and determination of estriol using a surfactant modified nanotube paste electrode. Eurasian J Anal Chem 14:1–11. https://doi.org/10.29333/ejac/20190101
67. Ashwini KS, Upadhyay SS, Rawool CR, Punde NS, Rajpurohit AS (2019) Voltammetric techniques for the analysis of drugs using nanomaterials based chemically modified electrodes. Curr Anal Chem 15:249–276. https://doi.org/10.2174/1573411014666180510152154
68. Tigari G, Manjunatha JG (2020) A surfactant enhanced novel pencil graphite and carbon nanotube composite paste material as an effective electrochemical sensor for determination of riboflavin. J Sci: Adv Mater Devices 5:56–64. https://doi.org/10.1016/j.jsamd.2019